

Mode Selection by Application of an External Signal in an Overmoded Gyrotron Oscillator

A. H. McCurdy^(a) and C. M. Armstrong

Naval Research Laboratory, Washington, D.C. 20375

(Received 19 November 1987)

Mode control is achieved for the first time in a highly overmoded, pulsed rf oscillator by injection of an external electromagnetic signal (priming). The drive signal power, frequency, and time of application determine the degree of mode control. The regime of parameter space over which a primed gyrotron operates in a single stable mode is increased by $\sim 40\%$. A coupled mode theory is used to model the drive power dependency of the priming effect. Priming may allow gyrotrons to operate at increased efficiency as well as stabilize other overmoded coherent radiation sources.

PACS numbers: 42.52.+x, 42.10.Mg, 85.10.Jz

As the frequency and power requirements on radiation sources in the microwave and millimeter wavelength range increase, the problems of mode competition become more severe.^{1,2} For example, all the oscillator concepts (gyrotron, free-electron laser, and variants) considered for fusion heating share this problem since the mode density scales as a power of d/λ , where λ is the operating wavelength and d is a characteristic dimension of the oscillator electrodynamic structure ($d \gg \lambda$ because of the high power density involved). In particular, the electron-cyclotron-resonance heating requirements for the compact ignition tokamak (CIT) are ~ 1 MW at a frequency of ~ 280 GHz. An oscillator meeting these performance specifications will have a frequency separation between modes which will at best be comparable to the gain bandwidth of the device. This raises the possibility of mode transitions, due to noise in the oscillator, as well as an inability to operate the oscillator at maximum efficiency.

The solution proposed in this Letter is to "prime" the desired mode by injecting an external rf signal into the oscillator during the oscillation buildup. Our examination of the efficacy of this approach involves (a) experimentally identifying the novel properties of this type of mode control, and (b) proposing and then comparing with experiment a simple model based on a multimode, quasilinear theory. Though termed "injection seeding" in the laser community,³ we show that this phenomenon is related to the previous work on oscillator priming⁴ and hence call it "mode priming."

The problem of mode competition in high performance gyrotrons is clear.^{2,5} The most successful means of gyrotron mode control, the complex cavity technique,⁶ is inflexible and presents design complications. In contrast, the mode primed system requires only a low-power drive source with a small frequency tuning range (several percent) and a suitable coupling scheme. Furthermore, the requirements on drive power and isolation may be reduced by injecting the drive into a separate cavity to premodulate the electron beam as demonstrated in the phase-locked gyrotron.⁷

The mode selection experiments are performed using a

5.0-GHz pulsed gyrotron oscillator. The gyrotron cavity (Fig. 1) is a cylindrical waveguide, with a radius of 1.75 cm and length of $\sim 10\lambda$, terminated by discontinuities at the electron gun and collector ends. The beam parameters are 20 kV at 2 A with a measured perpendicular-to-parallel velocity ratio of ~ 1.36 . Power is coupled out of the cavity via fourteen capacitively coupled disk probes and two inductive loop probes (inset Fig. 1). Because the probes are weakly coupled to the cavity, internal Ohmic losses cause the quality factors of the lowest four axial modes all to be ~ 1200 .

The characteristics of gyrotron operation, as calculated from single-mode linear theory,⁸ are shown in Fig. 2. The start oscillation current thresholds for the first three TE_{11n} modes are given as a function of magnetic field (I - B plane). Only the lowest magnetic field branch of each mode is shown. The similar (~ 0.02 A) start oscillation currents and the large overlap of regimes of excitation of the different modes suggest significant mode competition. The gyrotron gain bandwidth is 3 times the mode spacing and, because of the narrow transverse cavity dimension, there is only competition between axial modes.

In the experiment, the external signal is generated by a sweep oscillator and injected via phase shifters through

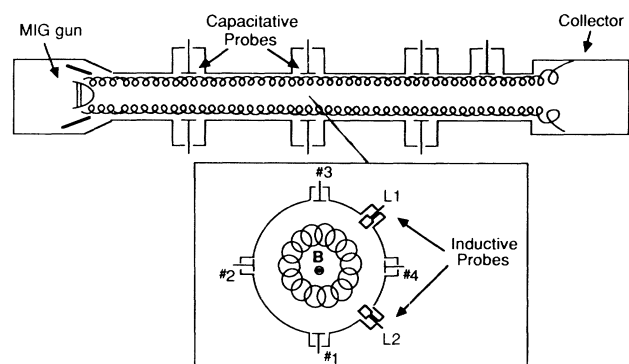


FIG. 1. Configuration of the gyrotron with inset showing midplane probe geometry.

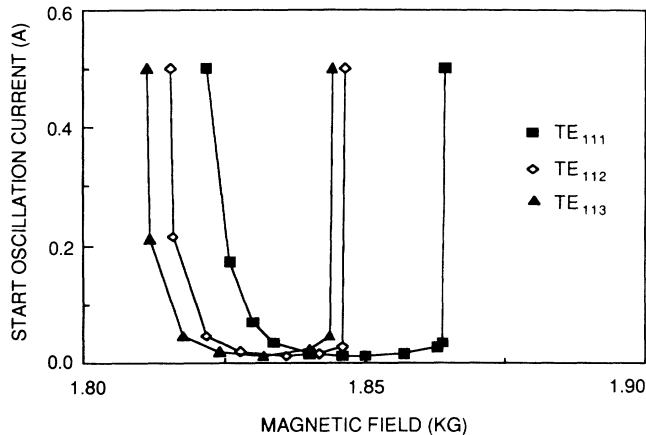


FIG. 2. Start oscillation current thresholds for the three lowest-order axial modes from single-mode linear theory.

probes 1 and 2 (see Fig. 1). The relative phase between probes may be chosen to excite a right-hand circularly polarized wave in the cavity. The gyrotron output rf is monitored through another probe (usually L1 or L2). The operating mode is determined in two ways: (a) from frequency measurements using a tunable bandpass filter in the gyrotron output and (b) measurement of the spatial field profile using the probes along the cavity axis. Measurements of gyrotron operation in the I - B plane reveal that a complicated pattern of pure modes separated by regions of pulse-to-pulse mode skipping exist in the free-running case. Application of the drive signal enables single-mode operation if the drive frequency is close to one of the modes. Figure 3 shows the nearly 40% expansion of pure TE_{111} mode operation in the I - B plane due to a priming signal. Since the probes weakly couple the drive signal to the cavity, the drive power inside the cavity amounts to only about 0.01% of the oscillator power. However, relating the drive power to the oscillator power is merely a figure of merit, since for a given set of oscillator parameters, the degree of mode priming directly depends on the relative size of the drive power and the preoscillation noise power. The regime of primed TE_{111} operation is found to displace free-running regimes of stable TE_{112} , TE_{114} , TE_{118} , and TE_{119} operation and regions of pulse-to-pulse mode skipping involving these and other modes. Other experiments show expansion of pure mode operation for the higher-order axial modes as well as for gyrotron operation at the second harmonic of the cyclotron frequency (TE_{21n} modes at ~ 8.5 GHz). This expansion of the region of pure mode operation may enhance gyrotron performance since the predicted regime of highest efficiency for a given mode typically occurs near the boundary of excitation of a competing mode.²

The dependence of the mode priming effect on the frequency separation between the drive signal and gyrotron has been briefly explored. The drive power required for

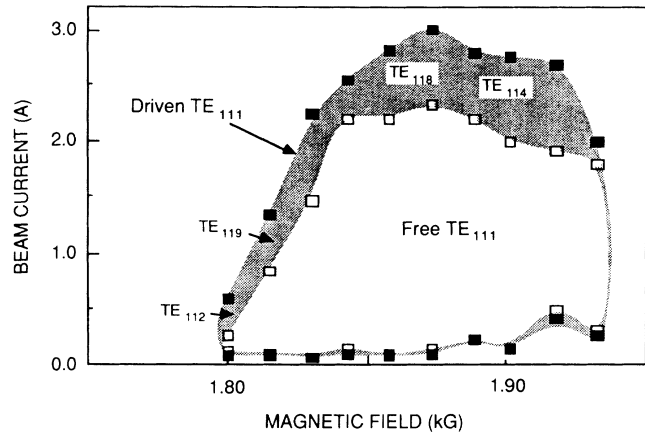


FIG. 3. Enlargement of region of pure TE_{111} mode oscillation due to a 20-W drive signal at the oscillation frequency (shaded). Regions of displaced pure mode operation are indicated.

a given level of control is found to increase exponentially with frequency separation. As is the case with phase priming,⁷ significant mode control can be obtained at frequency separations well outside the cavity resonance band (a factor of 3 or more). One unresolved issue is the observation that the drive frequency which exerts maximum control is slightly above that of the free-running oscillation.

The temporal dependence of the mode priming phenomenon is determined experimentally by applying a pulsed drive signal (50 ns wide) to the gyrotron. It is found that the drive signal only has an effect during a brief interval ~ 300 ns before the oscillation saturates. This dependence is also characteristic of phase priming.⁹ This feature may allow electronic isolation of the drive source from the gyrotron during the steady state to prevent damage due to feedback power.

The quantitative description of the mode priming phenomenon begins with the quasilinear, coupled mode theory of Lamb.¹⁰ This theory gives the temporal evolution of amplitudes and phases of a multiple mode system. The electron transit time through the cavity and the period of the rf radiation are assumed small compared to the time of amplitude growth of the oscillation. The weakly relativistic electron beam is assumed sufficiently tenuous so that the electron energy change (due to the rf electric field) around a Larmor orbit is small compared to the initial electron perpendicular kinetic energy. The modal frequency separation is greater than the cavity resonance width so that the modes interact solely through their amplitudes. The amplitude equations of motion (written in terms of power inside the cavity) are

$$dP_i/dt = P_i(\alpha_i - \beta_i P_i - \theta_{ik} P_k), \quad (1)$$

where $i, k = 1$ or 2 for two modes. P_i , α_i , and β_i , are the

power, the linear growth rate, and the self-saturation coefficient of the i th mode, respectively. θ_{ik} is the coefficient of cross saturation of mode i due to mode k . Our purpose is to extend this model to include noise and an external signal. In doing so we will use experimental values for the coefficients in Eq. (1) instead of calculating them exactly.¹¹

The linear growth rates are experimentally determined from crystal diode measurements of the gyrotron output power as a function of time. The self-saturation coefficients are found from the steady-state power levels, P_i^{sat} , using $\beta_i = \alpha_i/P_i^{\text{sat}}$. It is found experimentally (in all cases of interest here) that only one of two possible modes survives in the steady state; hence the cross-saturation coefficients must satisfy the criterion for strong coupling between modes ($\theta_{12}\theta_{21} > \beta_1\beta_2$). The cross-coupling coefficients are found from a numerical fit with the mode control experiment.

The calculated temporal evolution of modes with use of the experimentally determined coefficients is shown in Fig. 4. The system follows one of the trajectories from the initial conditions at the onset of oscillation (noise) to one of the two final steady-state power levels. The trajectory taken depends on the relative size of the preoscillation noise power in each mode. It has been verified previously that the preoscillation noise amplitude in a gyrotron varies statistically (from pulse to pulse) according to a Rayleigh distribution.⁹ Mode skipping can be interpreted in terms of this model as a result of the independent statistical variation in the preoscillation noise level of each mode from pulse to pulse causing a change in the trajectory that the system follows. The separatrix in Fig. 4 divides the trajectories which approach either

steady state and, near the origin, is described by the equation

$$P_2 = C P_1^{\alpha_2/\alpha_1}, \quad (2)$$

where $C = C(\alpha_1, \alpha_2, \beta_1, \beta_2, \theta_{12}, \theta_{21})$ is a constant which can be found numerically. The procedure by which this is accomplished begins with a linearization of Eq. (1) about the intersection of the lines $\alpha_i - \beta_i P_i - \theta_{ik} P_k = 0$. The equation for the separatrix near this point is a straight line with a slope that can be determined analytically. From this line, Eq. (1) can then be integrated backwards in time towards the origin. Near the origin a linear regression yields C .

The steady-state mode can be determined by the substitution of the initial power levels of the two modes in Eq. (2). If the left-hand side is greater than the right-hand side (the initial condition is *above* the separatrix), then the steady state will be mode 2. Otherwise mode 1 will prevail. The external drive signal is included by the modification of the initial condition from which the oscillation grows. This procedure is justified if the external signal is very small compared to the oscillation except during the earliest stages of buildup. A mode is selected by the application of the drive signal near the mode frequency with an amplitude such that the initial powers satisfy the criterion from Eq. (2). The noise power, due to cyclotron radiation,⁹ is simulated by randomly selecting (for each pulse) a noise amplitude for the undriven mode from a Rayleigh distribution. The amplitude of the driven mode is selected from a distribution found by adding the randomly phased, Rayleigh distributed noise vector to the drive signal.¹² The Rayleigh distribution mean is calculated from the measured mean noise power level of $0.3 \mu\text{W}$.⁹

The results of an experiment measuring the dependence of the degree of mode control on the external signal power level are shown in Fig. 5. Here the drive signal primes a TE_{111} mode from a pure free-running TE_{112} mode. The degree of mode control is found by measuring the fraction of missed gyrotron rf pulses (pulses not in the primed mode) out of a total of 250. It is found that the drive signal should be applied in the form of a right-hand circularly polarized wave for optimum control. This result is consistent with the fact that the electron cyclotron maser instability, upon which the gyrotron is based, is strongest for an electromagnetic wave rotating in the direction of the electrons. The curve in Fig. 5 is the predicted average fraction (averaged over 40 trials, with 250 pulses per trial) of missed pulses with the same coefficients as in Fig. 4. The θ_{ik} are found by fitting the theory to the free-running case and to one central data point. As the drive signal becomes large compared to the mean noise level (>1000 times) the gyrotron approaches a pure TE_{111} mode. The standard deviation of the missed pulse fraction over 40 trials, due to the random noise, is shown by the shading in Fig. 5. It can be

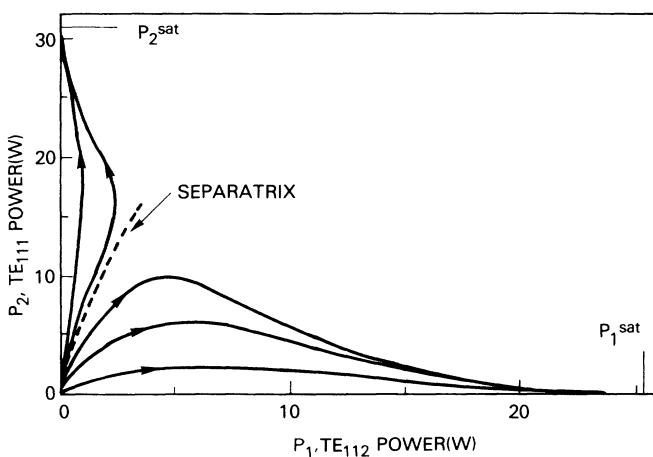


FIG. 4. Mode evolution for $\alpha_1 = 0.02 \text{ ns}^{-1}$, $\alpha_2 = 0.014 \text{ ns}^{-1}$, $\beta_1 = 7.86 \times 10^5 \text{ J}^{-1}$, $\beta_2 = 4.47 \times 10^5 \text{ J}^{-1}$, $\theta_{12} = 1.10 \times 10^6 \text{ J}^{-1}$, and $\theta_{21} = 2.05 \times 10^6 \text{ J}^{-1}$. This example models an experiment where mode 1 is TE_{112} and mode 2 is TE_{111} . The separatrix divides the trajectories approaching mode 1 from those of mode 2. Arrows indicate the direction of increasing time.

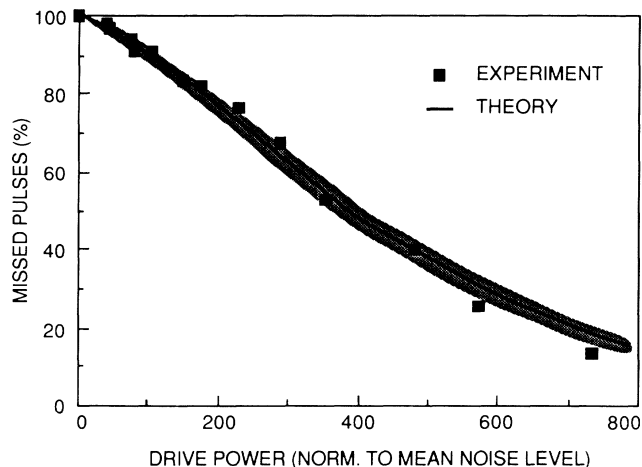


FIG. 5. Degree of mode control achieved with a given drive power and a $0.3\text{-}\mu\text{W}$ noise power. Shading shows the standard deviation in predicted control.

seen that most of the experimental points fall within the shaded region, indicating that the theory does predict, to within statistical uncertainties, the degree of mode control experimentally observed.

In summary, control of closely spaced axial modes in a gyrotron is achieved by modifying the initial condition from which the oscillation grows. A simulation of multimode oscillation growth agrees with the experimentally observed dependence of mode control on drive power level. We also show that the phenomenon of priming oscillator modes with an external signal is closely related to

priming of oscillator phase. The results presented here suggest a new method of obtaining mode control in microwave and millimeter-wave oscillators.

The authors thank B. McIntosh, F. Wood, and S. Swiadek for technical support. Support from S. Y. Park and R. K. Parker is also gratefully acknowledged. This work was sponsored by the Office of Naval Technology and the Office of Naval Research.

^(a)Present address: Omega-P Inc., 2008 Yale Station, New Haven, CT 06520.

¹L. R. Elias, G. Ramian, J. Hu, and A. Amir, *Phys. Rev. Lett.* **57**, 424 (1986).

²K. E. Kreischer and R. J. Temkin, *Phys. Rev. Lett.* **59**, 547 (1987).

³J. Lachambre, P. Lavigne, G. Otis, and M. Noël, *IEEE J. Quantum Electron.* **12**, 756 (1976).

⁴E. E. David, Jr., *Proc. IRE* **40**, 669 (1952).

⁵K. Felch *et al.*, in *Conference Digest of the Eleventh International Conference on Infrared and Millimeter Waves*, edited by G. Moruzzi (ETS Editrice, Pisa, Italy, 1986), p. 229.

⁶Y. Carmel *et al.*, *Phys. Rev. Lett.* **50**, 112 (1983).

⁷A. H. McCurdy *et al.*, *Phys. Rev. Lett.* **57**, 2379 (1986).

⁸K. E. Kreischer and R. J. Temkin, *Int. J. Infrared Millimeter Waves* **1**, 195 (1980).

⁹A. H. McCurdy and C. M. Armstrong, *IEEE Trans. Microwave Theory Tech.* **36**, 891 (1988).

¹⁰W. E. Lamb, Jr., *Phys. Rev. A* **134**, 1429 (1964).

¹¹G. S. Nusinovich, *Int. J. Electron.* **51**, 457 (1981).

¹²S. O. Rice, *Bell Sys. Tech. J.* **24**, 100 (1943).

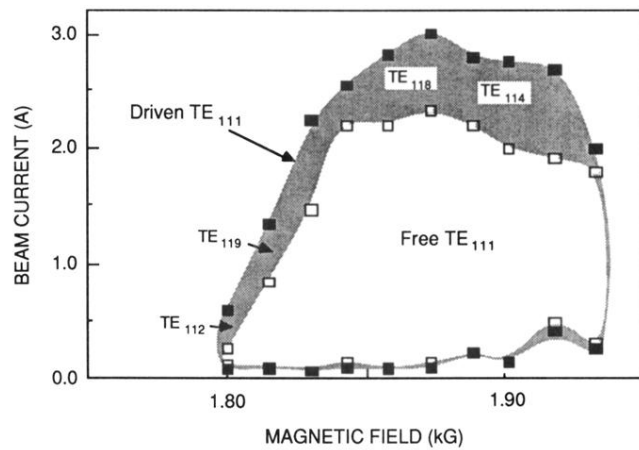


FIG. 3. Enlargement of region of pure TE₁₁₁ mode oscillation due to a 20-W drive signal at the oscillation frequency (shaded). Regions of displaced pure mode operation are indicated.

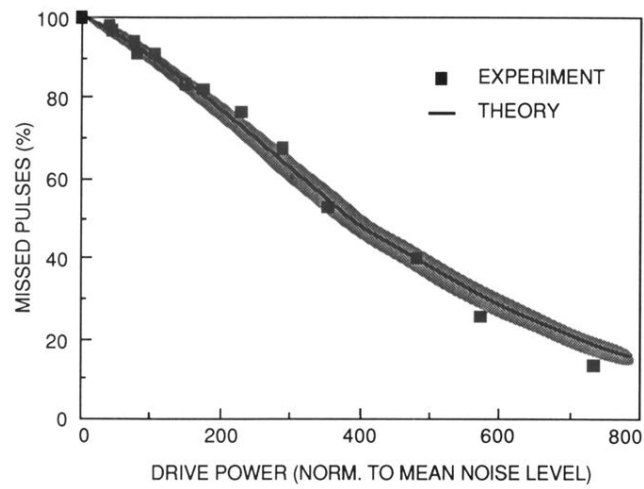


FIG. 5. Degree of mode control achieved with a given drive power and a $0.3\text{-}\mu\text{W}$ noise power. Shading shows the standard deviation in predicted control.